FIRST DRAFT

Deconvolution and Translation Between High Spectral Resolution IR Sounders

Howard E. Motteler

UMBC Atmospheric Spectroscopy Lab
Joint Center for Earth Systems Technology

October 2, 2015

1 Introduction

Upwelling infrared radiation as measured by the AIRS, IASI, and CrIS sounders is a significant part of the long term climate record. We would like to treat this information as a single data set but the instruments have different spectral resolutions, channel response functions, and band spans. As a first step in addressing this problem we consider several channel radiance translations: IASI to high resolution CrIS, IASI to AIRS, AIRS to standard resolution CrIS, and high resolution CrIS to AIRS.

Translation from AIRS to CrIS presents a special challenge because CrIS and IASI are Michaelson interferometers with parametrized response functions, while AIRS is a grating spectrometer with channel center frequencies and spectral response functions determined by the focal plane geometery. In section 6 we show how to take advantage of detailed knowledge of the AIRS spectral response function (SRF) shapes to deconvolve AIRS channel radiances to a resolution enhanced intermediate representation.

The translations presented here are validated by comparisons with calculated reference truth. For example to test the IASI to AIRS translation, we start with 49 fitting profiles spanning a significant range of atmospheric conditions. Upwelling radiance is calculated at a 0.0025 cm^{-1} grid with kcarta over a band spanning the AIRS and IASI response functions. "True AIRS" is calculated from this by convolving the kcarta radiances with tabulated AIRS SRFs, and "true IASI" by convolving kcarta radiances to the IASI instrument specs. IASI is translated to AIRS (we call this "IASI AIRS") and this is compared with true AIRS.

This sort of validation assumes perfect knowledge of the AIRS and IASI instrument response functions and so gives only a lower bound on how well the translations can work in practice. But the better we know the response functions, the closer practical translations can approach these limits.

The conversions here are presented in order of their residuals, with IASI to high resolution CrIS most accurate and high resolution CrIS to AIRS the least.

2 IASI to high resolution CrIS

The CrIS user grid comprises three bands, LW 650 to 1095 cm^{-1}, MW 1210 to 1750 cm^{-1}, and SW 2155 to 2550 cm^{-1}. For the CrIS high resolution mode the channel spacing is 0.625 cm^{-1} for all three bands. The CrIS user ILS is a sinc function. The IASI user grid is a single band from 645 to 2760 cm^{-1} with a channel spacing of 0.5 cm^{-1}. The IASI user ILS is a sinc function convolved with the modified Gaussian, shown in figure 1.

IASI to CrIS is a relatively easy translation because IASI spans the CrIS bands and has a nominal (though strongly apodized) higher resolution. The main steps of the translation, for each CrIS band, are

- apply a bandpass filter to the IASI channel radiances to restrict them to a single CrIS band with a roughly 20 cm^{-1} rolloff outside the CrIS user grid. For the LW band we use a 5 cm^{-1} rolloff because IASI starts at 645 cm^{-1}.
- take the filtered radiances to an interferogram with an inverse Fourier transform
- apply the pointwise inverse of the IASI Gaussian over the IASI 1 cm OPD and truncate this to the 0.8 cm CrIS OPD.

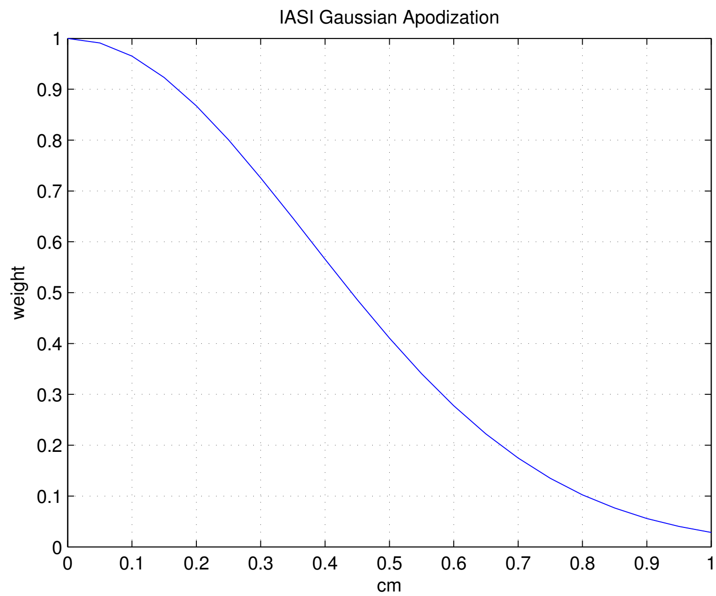

Figure 1: IASI truncated Gaussian apodization

- take the interferogram back to radiance at the CrIS 0.625 cm^{-1} channel spacing with a forward Fourier transform

Figure 2 shows the mean and standard deviation of IASI CrIS minus true CrIS for the 49 fitting profiles, for the CrIS LW band. The residual is greatest at the low end of the LW band. This may be due in part to the 5 cm^{-1} LW rolloff, as residuals near the band edges are larger with a smaller rolloff. The residual is reduced significantly if we apply Hamming apodization to the IASI CrIS and true CrIS radiances, as shown in figure 3. Figures 4 and 5 show similar results for the unapodized radiances for the MW and SW bands. The residuals are very small. Unless otherwise noted, all CrIS spectra shown here are unapodized.

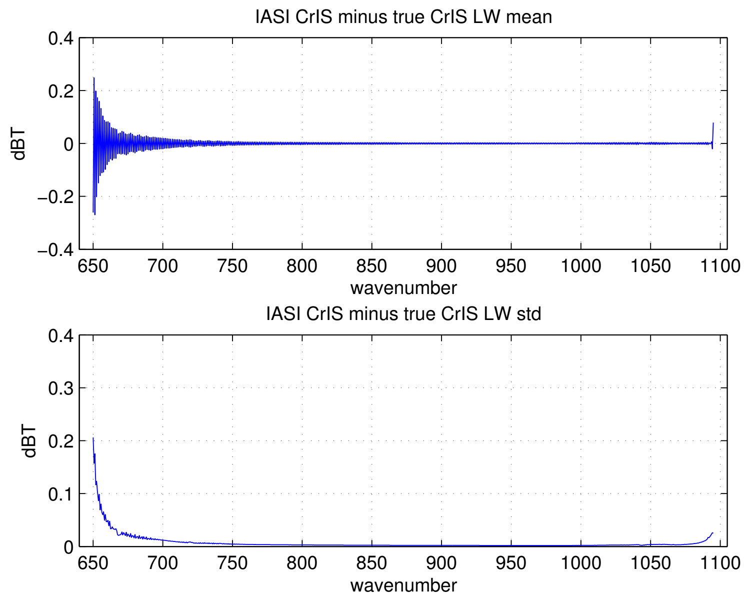

Figure 2: Mean and standard deviation of unapodized IASI CrIS minus true CrIS, for the CrIS LW band.

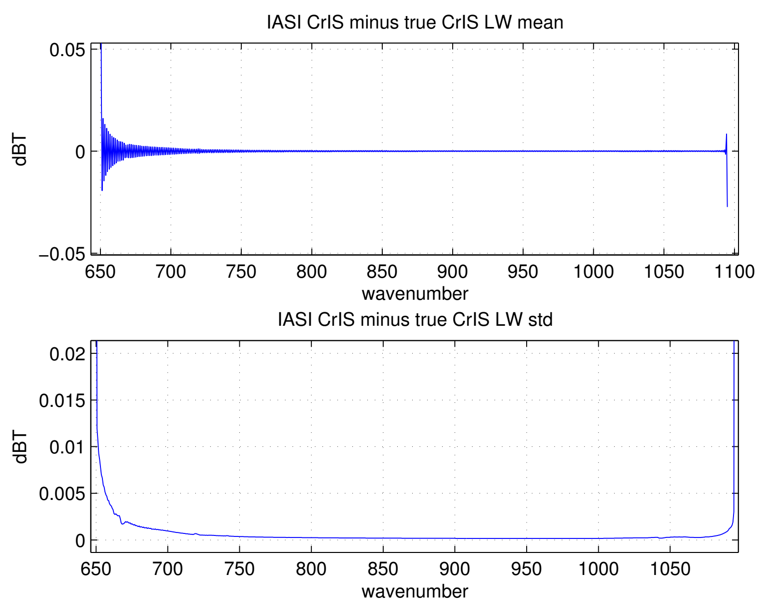

Figure 3: Mean and standard deviation of Hamming apodized IASI CrIS minus true CrIS, for the CrIS LW band.

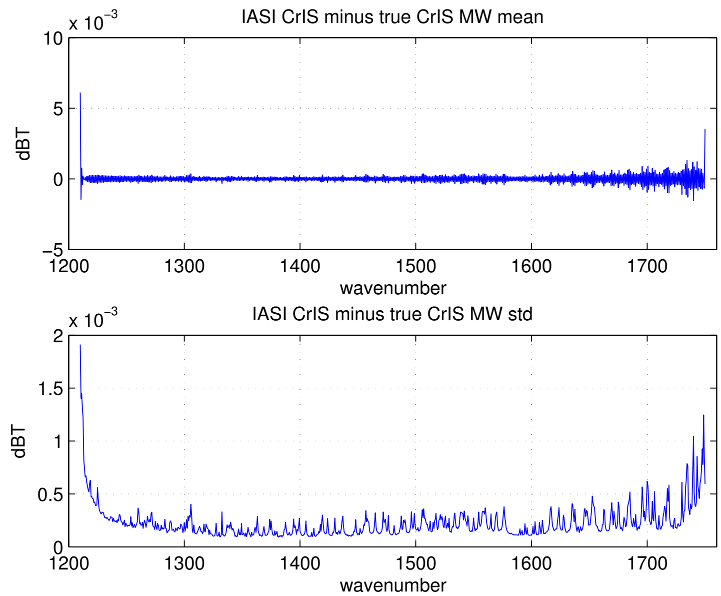

Figure 4: Mean and standard deviation of unapodized IASI CrIS minus true CrIS, for the CrIS MW band.

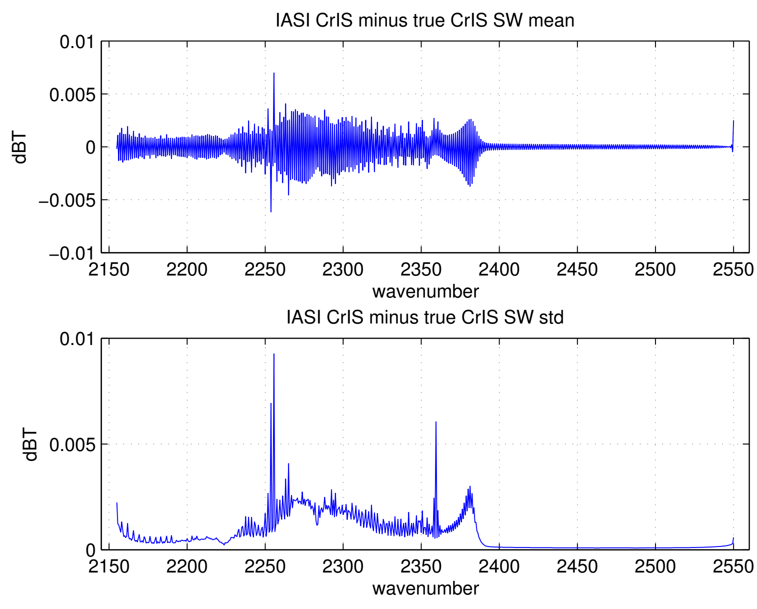

Figure 5: Mean and standard deviation of unapodized IASI CrIS minus true CrIS, for the CrIS SW band.

3 IASI to AIRS

AIRS L1b radiances are a set of channels between approximately 650 to 2650 cm^{-1} with the individual center frequencies and spectral response functions (SRFs) determined by the focal plane geometery. Channels are not uniformly spaced. AIRS L1c radiances are derived from the L1b with improvements including a more uniform spacing. The IASI to AIRS translation works for either channel set and is done as follows

- apply a bandpass filter to the IASI radiances to restrict them to the AIRS band span, with a 5 cm^{-1} rolloff
- deconvolve the filtered IASI radiances to a 0.1 cm^{-1} intermediate grid, the nominal resolution of the AIRS SRF tabulation. Aside from resolution and band spans, this exactly the same transform used for the IASI to CrIS translation and is done with the same procedure, iasi_decon.m
- convolve the 0.1 cm^{-1} intermediate representation with either the AIRS L1b or L1c SRFs. Section 6 discusses this convolution in greater detail.

Figure 6 shows the first three AIRS SRFs and the bandpass filter wing. Note the relatively gentle slope of the rolloff, to decrease impulse ringing. The first two AIRS SRFs are "guard channels" and the third the first regular channel. The wings of the SRFs roll off well inside the bandpass filter.

Figure 7 shows true IASI, true AIRS, deconvolved IASI, and IASI AIRS. At this level of detail we mainly see the greater fine structure in the deconvolution. Figure 8 shows details from 660 to 680 cm^{-1}. Figure 9 shows IASI AIRS minus true AIRS. The residual is larger than for the IASI to CrIS translation, but significantly better than the AIRS to CrIS or CrIS to AIRS translations.

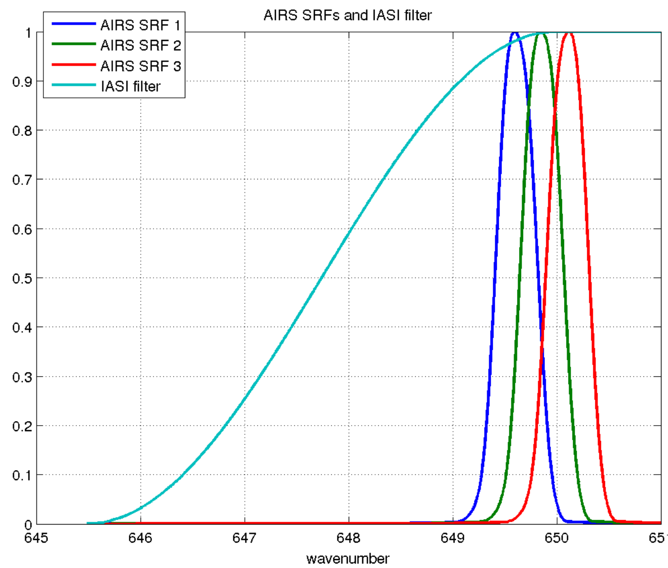

Figure 6: The first three AIRS SRFs and the bandpass filter wing

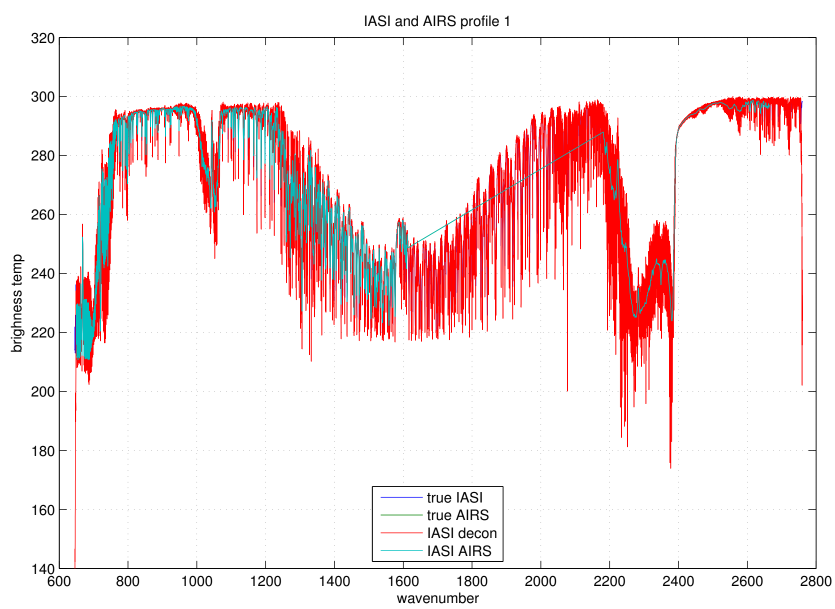

Figure 7: true IASI, true AIRS, deconvolved IASI, and IASI AIRS

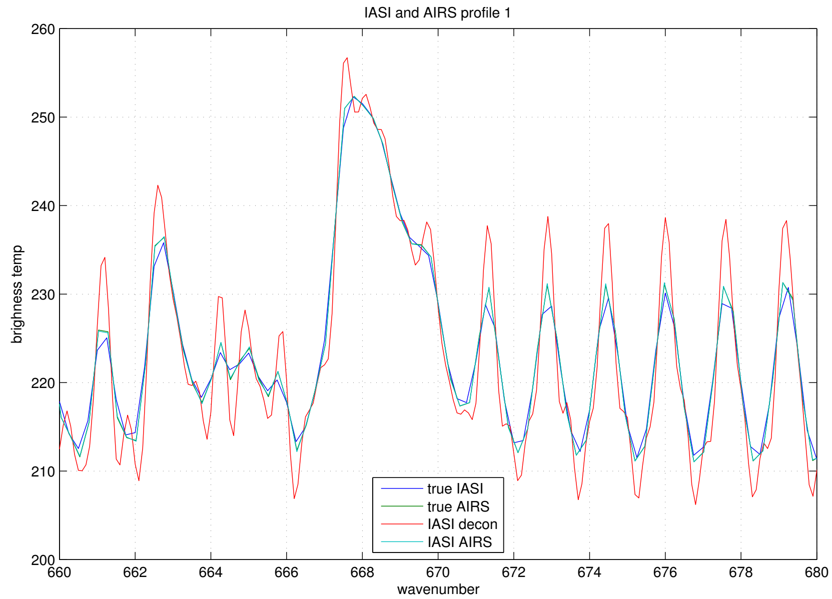

Figure 8: true IASI, true AIRS, deconvolved IASI, and IASI AIRS, detail

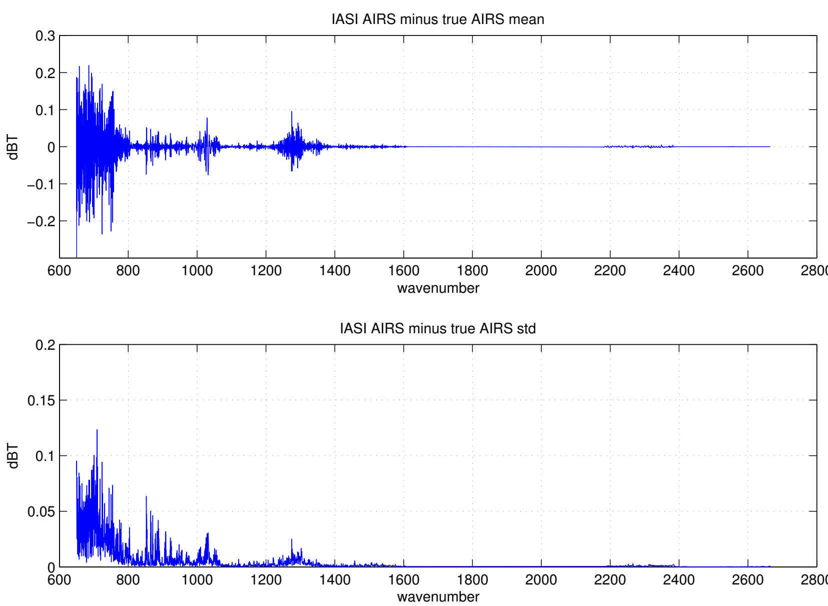

Figure 9: Mean and standard deviation of IASI AIRS minus true AIRS

4 AIRS to standard resolution CrIS

For the CrIS standard resolution mode the channel spacing is 0.625 cm^{-1} for the LW, 1.25 cm^{-1} for the MW, and 2.5 cm^{-1} for the SW bands. The IASI deconvolution was a key step in the IASI to CrIS and IASI to AIRS translations. Similarly, AIRS deconvolution is central to the AIRS to CrIS translation and is presented in detail in section 6. The first step in the AIRS L1c to CrIS translation is to deconvolve the AIRS L1c channel radiances to a 0.1 cm^{-1} intermediate grid, the nominal AIRS SRF resolution. Then for each CrIS band,

- find the AIRS and CrIS band intersection
- apply a bandpass filter to the deconvolved AIRS radiances to restrict them to the intersection, rolling off the wings when the AIRS band and gaps allow for this
- reconvolve the filtered spectra to the user grid channel spacing for the current CrIS band
- trim the reconvolved spectra to the band intersection

Figure 10 shows true CrIS, true AIRS, deconvolved AIRS, and AIRS CrIS. At this level of detail we mainly see the greater fine structure in the deconvolution. Figure 11 shows details from 660 to 680 cm^{-1}. In comparison with the IASI deconvolution in figure 8 the AIRS deconvolution is not as smooth. The remaining figures show true CrIS minus AIRS CrIS for the 49 fitting profiles, with and without Hamming apodization for each of the CrIS bands. The residuals are significantly reduced with apodization but are larger than for the IASI to CrIS translation.

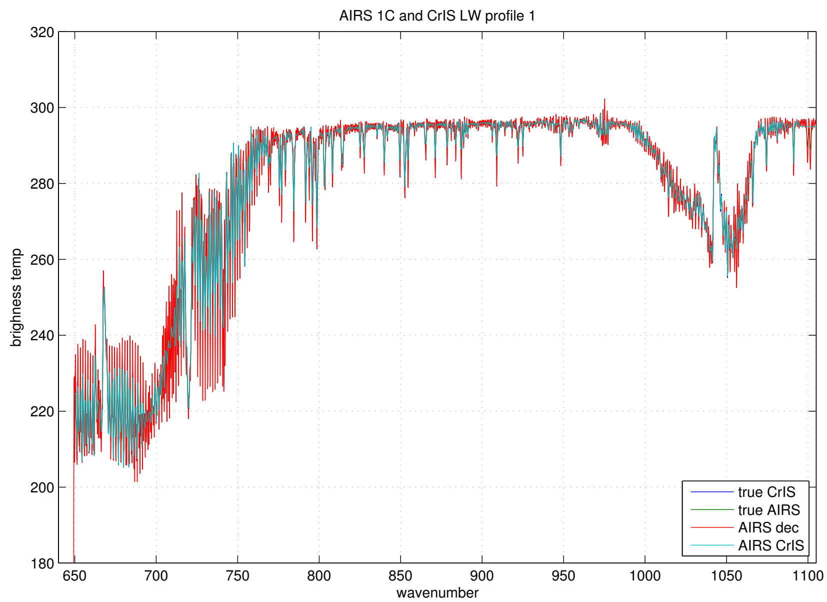

Figure 10: true CrIS, true AIRS, deconvolved AIRS, and AIRS CrIS

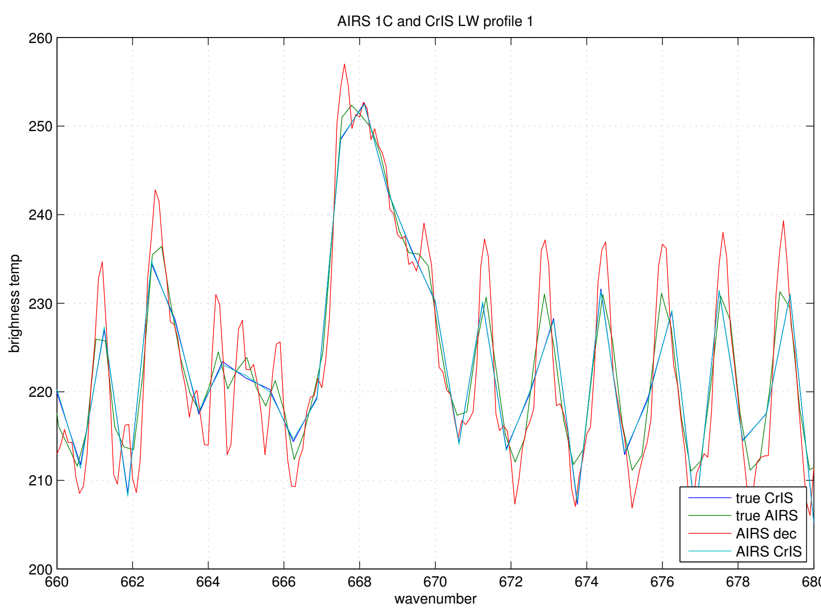

Figure 11: true CrIS, true AIRS, deconvolved AIRS, and AIRS CrIS, detail

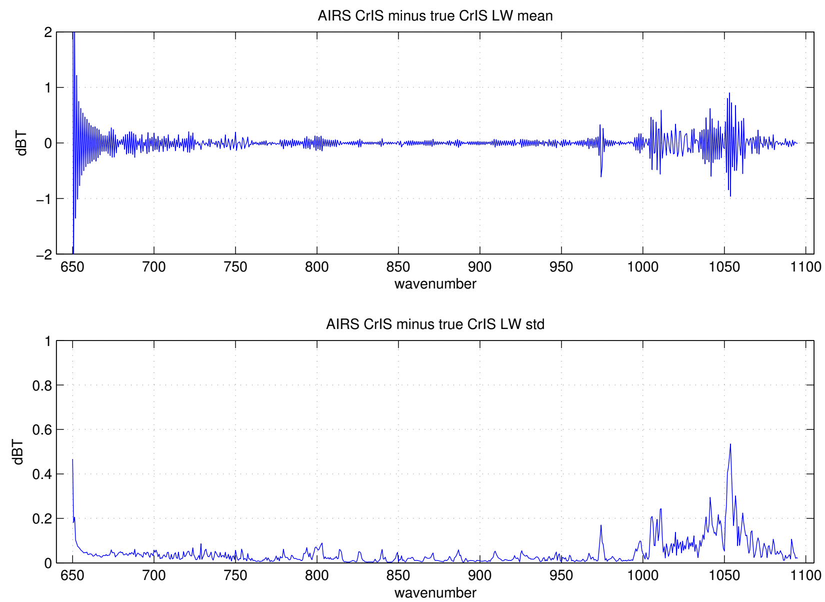

Figure 12: Mean and standard deviation of unapodized AIRS CrIS minus true CrIS, for the CrIS LW band

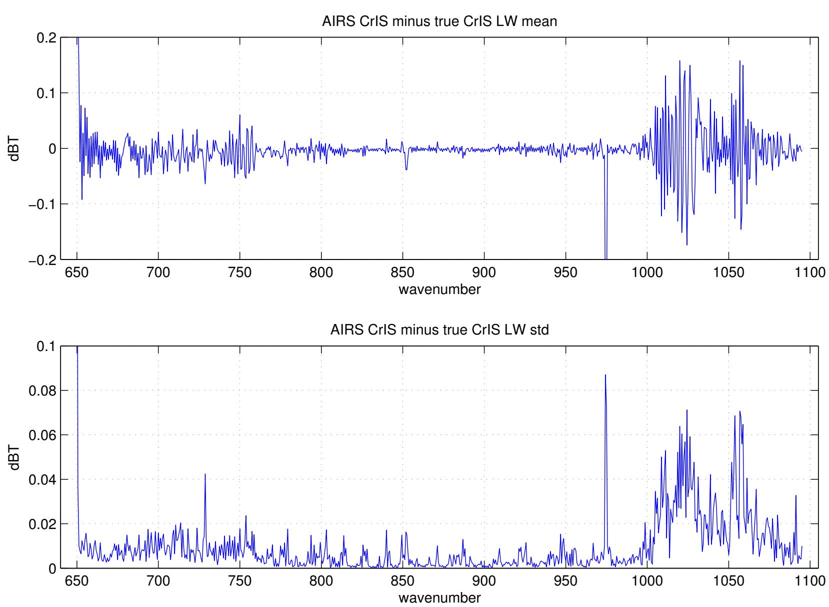

Figure 13: Mean and standard deviation of Hamming apodized AIRS CrIS minus true CrIS, for the CrIS LW band

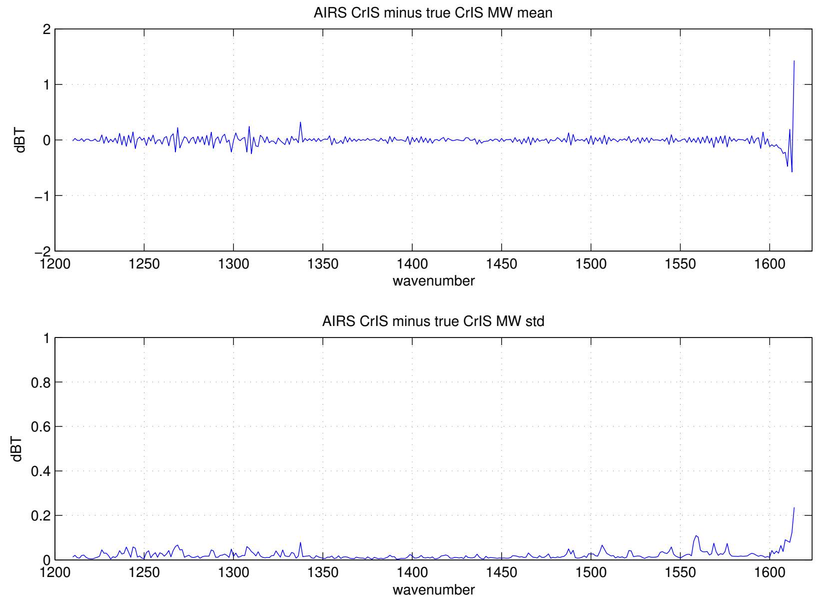

Figure 14: Mean and standard deviation of unapodized AIRS CrIS minus true CrIS, for the CrIS MW band

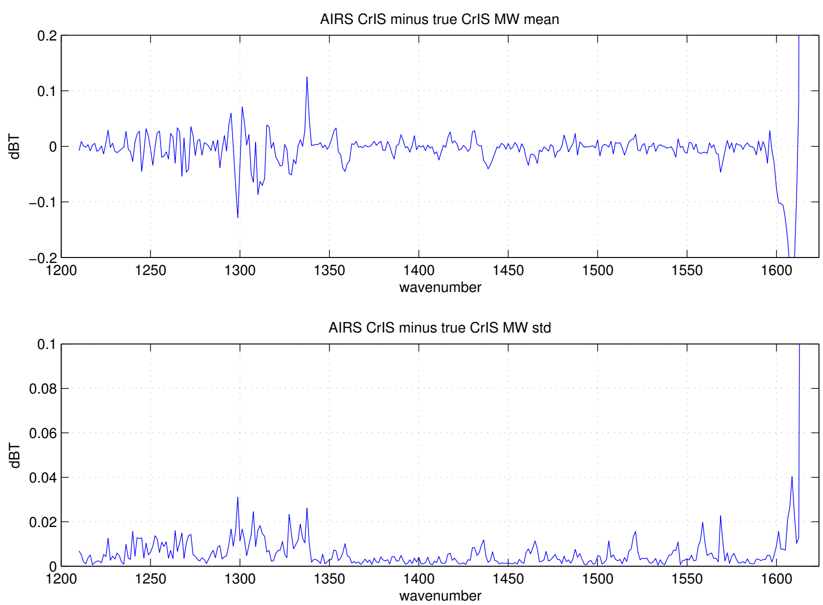

Figure 15: Mean and standard deviation of Hamming apodized AIRS CrIS minus true CrIS, for the CrIS MW band

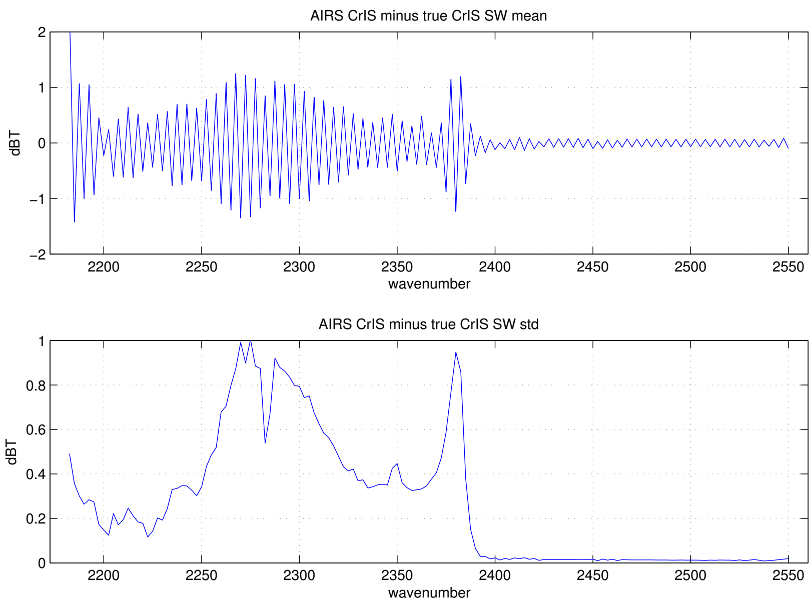

Figure 16: Mean and standard deviation of unapodized AIRS CrIS minus true CrIS, for the CrIS SW band

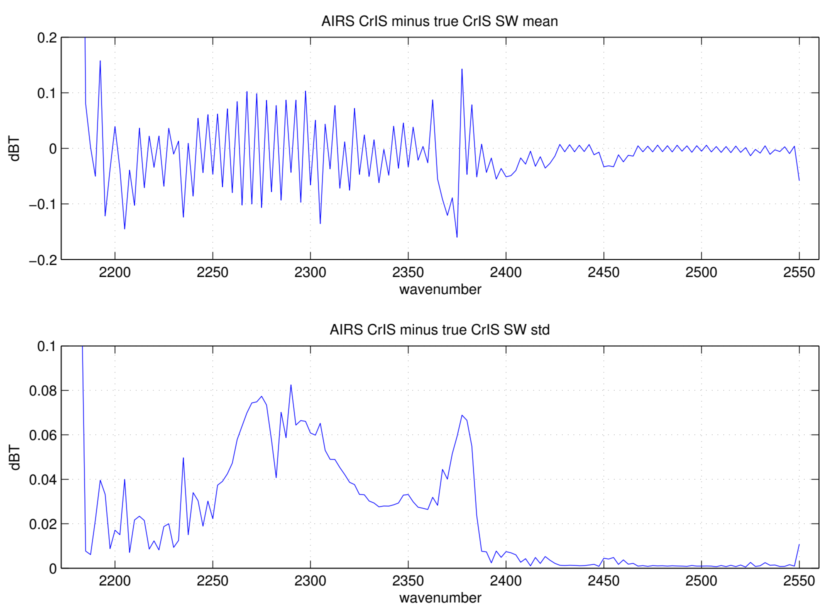

Figure 17: Mean and standard deviation of Hamming apodized AIRS CrIS minus true CrIS, for the CrIS SW band

5 High resolution CrIS to AIRS

The CrIS to AIRS translation differs in that we construct the intermediate representation at the 0.1 cm^{-1} AIRS SRF resolution by double Fourier interpolation, as the CrIS user grid sinc ILS does not allow for deconvolution. For each CrIS band, the steps in the translation are as follows,

- find the AIRS and CrIS band intersection
- interpolate the CrIS channel radiances to the intermediate grid
- convolve the 0.1 cm^{-1} intermediate representation with either the AIRS L1b or L1c SRFs

Note that there is no bandpass filtering used in this translation. For example in the LW we simply interpolate the full span of the CrIS user grid (plus any guard channels) to the intermediate representation. Adding a rolloff inside the user grid would improve residuals near the band edges but would mean dropping channels from the translation.

Figure 18 shows true CrIS, true AIRS, interpolated CrIS, and CrIS AIRS. Figure 19 shows details from 660 to 680 cm^{-1}. We do not see the resolution enhancement in the intermediate representation that we got with the IASI and AIRS deconvolutions. Figure 20 shows CrIS AIRS minus true AIRS. The residual is quite large in comparison with the other translations.

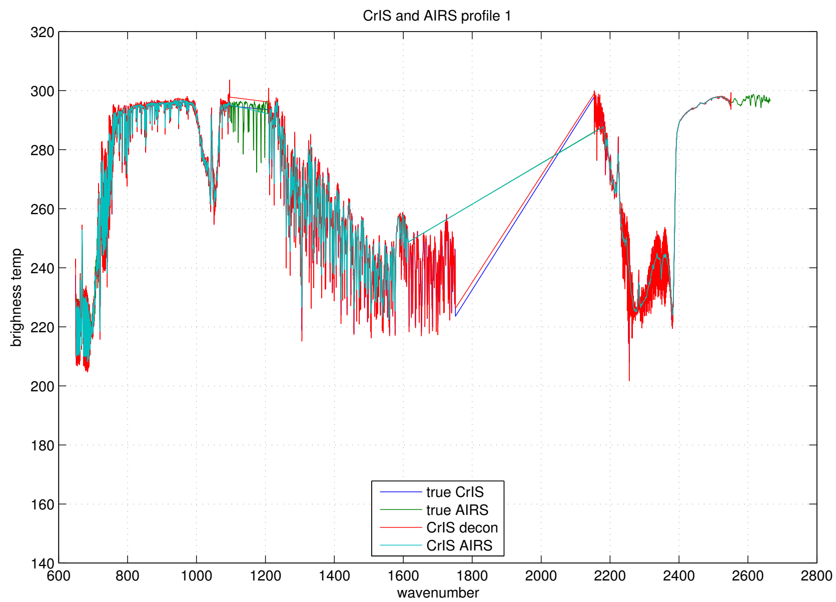

Figure 18: true CrIS, true AIRS, interpolated CrIS, and CrIS AIRS

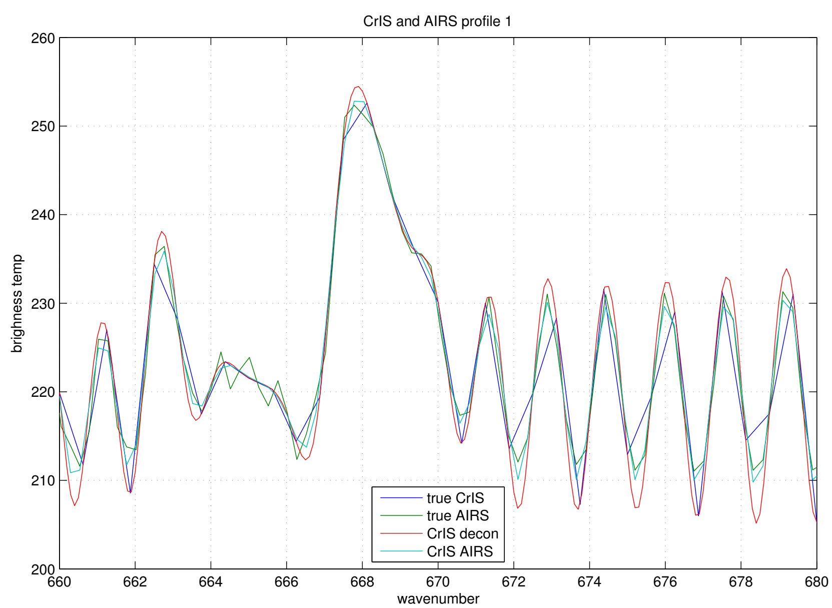

Figure 19: true CrIS, true AIRS, interpolated CrIS, and CrIS AIRS, detail

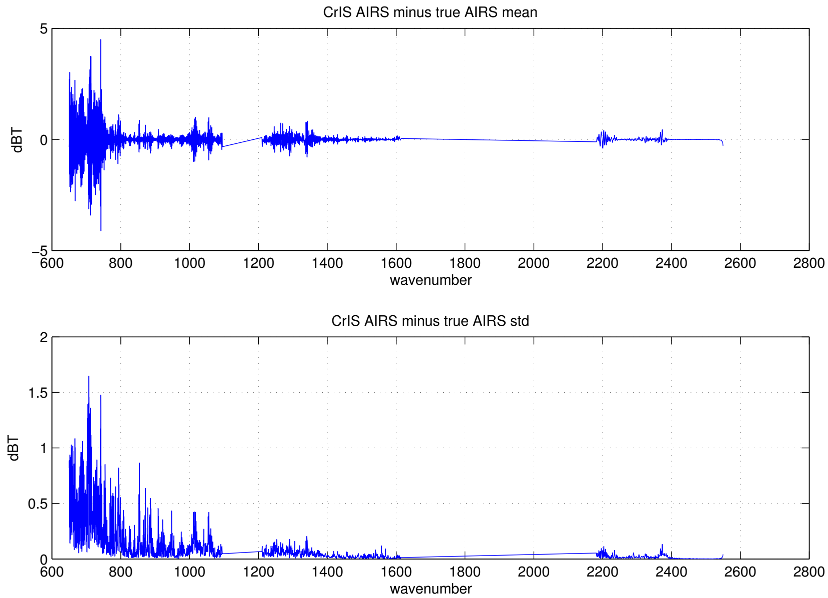

Figure 20: Mean and standard deviation of CrIS AIRS minus true AIRS

6 AIRS Deconvolution

The AIRS spectral response functions model channel response as a function of frequency and associate channels with nominal center frequencies. Each AIRS channel i has an associated spectral response function or SRF $\sigma_i(v)$ such that the channel radiance $c_i = \int \sigma_i(v) r(v)\, dv$, where r is radiance at frequency v. The center or peak of σ_i is the channel frequency.

Suppose we have n channels and a frequency grid $\mathbf{v}$ of k points spanning the domains of the functions σ_i. The grid step size for our applications is often 0.0025 cm^{-1}, the kcarta resolution. Let S_k be an $n \times k$ array such that $s_{i,j} = \sigma_i(v_j)/w_i$, where $w_i = \sum_j \sigma_i(v_j)$, that is where row i is $\sigma_i(v)$ tabulated at the grid $\mathbf{v}$ and normalized so the row sum is 1. If the channel centers are in increasing order S_k is banded, and if they are not too close, the rows are linearly independent. S_k is a linear transform whose domain is radiance at the grid $\mathbf{v}$ and whose range is channel radiances. If r is radiance at the grid $\mathbf{v}$, then $c = S_k r$ gives a good approximation of the channel radiances $c_i = \int \sigma_i(v) r(v)\, dv$.

In practice this is how we convolve kcarta or other simulated radiances to get AIRS channel radiances. We construct S_k either explicitly or implicitly from AIRS SRF tabulations. The matrix S_k in the former case is large but managable with a banded or sparse representation.

Suppose we have S_k and channel radiances c and want to find r, that is, to deconvolve c. Consider the linear system $S_k x = c$. Since $n < k$ for the kcarta grid mentioned above this is underdetermined, with infinitely many solutions. We could add constraints, take a pseudo-inverse, consider a new matrix S_b with columns tabulated at some coarser grid, or some combination of the above. We consider two cases, S_a with SRFs tabulated at the AIRS channel grid, and S_b with SRFs at an intermediate grid, typically 0.1 cm^{-1}, the approximate resolution of the SRF measurements.

6.1 Deconvolution to the AIRS channel grid

Let $\mathbf{v}_a = v_1, v_2, \ldots, v_n$ be channel center frequencies associated with a set of SRFs. Similar to S_k, let S_a be an $n \times n$ array where row i is $\sigma_i(v)$ tabulated at the v_a grid, with rows normalized to 1. If r is radiance at the grid $\mathbf{v}_a$, then $c = S_a r$ is a rough approximation of $\int \sigma_i(v) r(v)\, dv$.

Consider the linear system $S_a x = c$, similar to the case $S_k x = c$ above, where we are given S_a and channel signals c and want to find radiances x. Since S_a is an $n \times n$ matrix we might hope to solve for r. However in practice there are problems. If we take $\mathbf{v}_a$ as the standard AIRS L1b channel set, we find S_a is poorly conditioned, without a usable inverse. This is due to the L1b channel spacing, which because of module overlaps is quite variable, with the closest channels only 0.0036 cm^{-1} apart.

If we use the the linear function $g(v) = 4 \cdot 10^{-4} \cdot v - 0.04$, where v is frequency, as a lower bound on the acceptable channel spacing, we drop about 64 out of the 2378 L1b channels and the condition number of S_a is much improved, to around 30. With the partly synthetic L1c channel set, $g(v)$ drops only 4 channels and $\mathrm{cond}(S_a)$ is about 250, still low enough to get a usable inverse. The higher condition number for the L1c channel set is not surprising since the extra channels are synthesized from the L1b set.

6.2 Deconvolution to the SRF tabulation grid

We now consider deconvolution to an intermediate grid, 0.1 cm^{-1}, the resolution of the tabulated AIRS SRFs. Let $\mathbf{v}_b = v_1, v_2, \ldots, v_m$ be a 0.1 cm^{-1} grid spanning the domains of the functions σ_i. Similar to S_k, let S_b be an

$n \times m$ array where row i is $\sigma_i(v)$ tabulated at the $\mathbf{v}_m$ grid, with rows normalized to 1. If r is radiance at the $\mathbf{v}_b$ grid, then $c = S_b r$ is still a reasonable approximation of $\int \sigma_i(v) r(v)\, dv$.

Consider the linear system $S_b x = c$, similar to the case $S_k x = c$ above, where we are given S_b and channel signals c and want to find radiances x. Since $n < m < k$, as with S_k the system will be underdetermined but more manageable because m is approximately 40 times less than k. After trying several approaches we settled on a Moore-Penrose pseudoinverse S_b^{-1} of S_b. Given that, $x = S_b^{-1} c$ gives us deconvolved radiances at the SRF tabulation grid. This is what we use for the AIRS to CrIS translation in section 4.

6.3 Notes

- The work evolved as described above, with deconvolution to the AIRS channel grid a key step in getting deconvolution to the SRF tabulation grid to work. But rather than the AIRS channel grid it might be simpler to deconvolve to n regularly spaced points spanning the SRF domains, and check the condition number and get the channel spacing from that.

- Some of the earlier blog posts include comparisons of deconvolution based translation with both regular interpolation and translation to an intermediate grid with interpolaton rather than deconvolution. This is an important motivation for the deconvolution based translations.

- It may be possible to use a sinc basis for the intermediate representation and turn the deconvolution from an under- to an over-determined system that can be solved by regression. I have notes on this but didn't pursue it because the pseudo-inverse based deconvolution was working fairly well.